JOURNAL OF CATALYSIS 153, 32–40 (1995)

Performance of Heterogeneous Photocatalytic Systems: Influence of Operational Variables on Photoactivity of Aqueous Suspension of TiO_2

Vincenzo Augugliaro, Vittorio Loddo, Leonardo Palmisano, and Mario Schiavello

Dipartimento di Ingegneria Chimica dei Processi e dei Materiali, Università di Palermo, Viale delle Scienze, 90128 Palermo, Italy

Received June 8, 1994; revised November 2, 1994

The influence of incident light intensity and of some physical and chemical parameters on the absorbed and backward reflected photon flow and on the reactivity of a heterogeneous photocatalytic system was investigated. The oxidation of phenol in aqueous solution in the presence of polycrystalline TiO_2 powder was used as a test reaction. Home-prepared TiO_2 (anatase) specimens, subjected to various thermal treatments, were used for the experimental runs performed in a batch photoreactor directly irradiated. The physical parameters investigated were the surface area and the size of particles, while the chemical parameters studied were the initial pH of the suspension and the presence in the reacting medium of additives affecting the photoreactivity such as Cl^- and H_2O_2. It was found that the ratio between backward reflected and incident photon flow does not depend on the used operative variables, while the apparent Napierian extinctance coefficient, which is a parameter related to the photon absorption rate, depends only on the particle size and decreases as the particle size increases. The photoreaction quantum yield, defined as the ratio between the phenol reaction rate and the photon absorption rate, was determined for the various experimental conditions used in this work. The results showed that at equivalent conditions the quantum yield is an intrinsic feature of the semiconductor material; the quantum yield varies only by varying the reaction rate which, in our case, was affected only by the initial pH of the suspension and by the presence of Cl^- and H_2O_2. © 1995 Academic Press, Inc.

INTRODUCTION

Heterogeneous photocatalysis by semiconductor powders is a recent method proposed for the decontamination treatment of waste water effluents (1–3). In this way many organic contaminants can be degraded into nontoxic compounds such as carbon dioxide, water, and mineral acids.

The basic principles of photocatalyzed redox processes have been extensively investigated but the applied research for the development of these systems is to date unsatisfactory. There is not general agreement on which quantities are to be measured for a correct comparison of the performance of different photocatalytic systems (4–8). These systems are affected by the irradiation conditions and by the photoreactor features. In order to develop realiable models, the intrinsic kinetics of the photoreacting system, in which electrochemical and catalytic phenomena are occurring, must be known. The kinetics are affected in a nonlinear way by the radiation distribution inside the heterogeneous system in which light scattering (together with the chemical reaction) occurs.

A photocatalytic system for water treatment usually consists of semiconductor particles in contact with an aqueous solution containing organic compounds. The solid photocatalyst is generally used as a fine powder or is supported on another material. The irradiation in the near-UV region of such a system determines an environment in which redox reactions of degradation can take place.

Titanium dioxide (anatase) is widely used as photocatalyst owing to its (photo)chemical stability, high efficiency and low cost (9). TiO_2 is a semiconductor of wide band gap (E_g = 3.2 eV) and absorbs light with wavelength below ca. 390 nm. A very favorable feature of this semiconducting metal oxide is that the photogenerated holes have high positive oxidation potentials and, therefore, are able to oxidize most organic compounds to carbon dioxide and mineral acids (10, 11).

In this paper the influence of several operational variables on the optical properties of TiO_2 suspensions and on the activity of this system for a test reaction, namely, phenol photodegradation, has been investigated. In particular the following parameters have been studied: light intensity, specific surface area, particle size, pH of the suspension, presence of chloride ions, and hydrogen peroxide in the reacting medium. Aqueous suspensions of "home-prepared" polycrystalline TiO_2 (anatase) of satisfactory mechanical strength have been used for the phenol photodegradation. This reacting system is well known both from a kinetic and a mechanistic point of view (12–15) so that it is particularly useful to be used as a test reaction.

0021-9517/95 $6.00

The optical characterization of the suspension has been performed by using an experimental method (16, 17), which allows one to determine the absorbed and reflected photon flows by only measuring the incident and transmitted photon flows. The previous measurements also allow the determination of an optical property of the suspension, the apparent Napierian extinctance (ANE). The ANE, as stated very clearly by Martin *et al.* (18), is a phenomenological parameter which is useful for comparing experimental results obtained with the same experimental setup.

The quantitative comparison of the performance of the system under the various experimental conditions used in this work has been done by determining two quantities: (a) the turnover frequency, defined as phenol molecules reacting per unit of time and surface area of catalyst; and (b) the absorbed photon flux, defined as photons absorbed per unit of time and surface area of catalyst. From the knowledge of the above quantities, the kinetic constant of the rate equation and the quantum yield (qy) of photoreaction, defined as the ratio between reacted molecules and absorbed photons, have been calculated and consequently used for comparing the different systems.

EXPERIMENTAL

The experimental apparatus was made of two cylindrical vessels (i.d. = 58 mm) of Pyrex glass, vertically positioned one on top of the other; the upper vessel contained the aqueous TiO_2 suspension, and the lower one an actinometer solution. The external surfaces of both vessels were covered by mirror-polished aluminum sheets while a Pyrex sheet was placed on top of the upper vessel. All the apparatus was kept inside a box with black internal walls in which an oxygen atmosphere was maintained. The photoreactor was directly irradiated from the circular top surface of the upper vessel. The arc lamp supply (8540 Oriel Corp., USA) was furnished by a 1000- or a 500-W Hg–Xe lamp (L 5173 and 6285, Hanovia) and by a system of collimating lenses. The distance between the lenses and the top of the suspension was always 71 cm. A water filter was present in the illuminator so that IR radiation was cut off. The temperature of the reacting system was checked and it was about 308 K for all the experiments. In order to change the radiation intensity impinging on the system, Pyrex sheets of different thicknesses were interposed between the collimating lenses and the photoreactor. In this way five series of experimental runs were carried out at the following light intensities: 10.85×10^{-8}, 4.17×10^{-7}, 4.54×10^{-7}, 5.0×10^{-7}, and 2.75×10^{-6} einstein $\times$ s^{-1}.

For each light intensity used two different series of experimental runs were carried out: the first ones were performed for determining the transmitted photon flow, Φ_0, as a function of the suspension volumes (16, 17). The following volumes of aqueous suspension were used: 40, 50, 60, 70, 75, and 80 cm^3. These runs, which lasted 30 s, were carried out by using a TiO_2 concentration of 10^3 g $\times$ m^{-3} in the presence of a phenol concentration of 20 g $\times$ m^{-3}. The pH's of the suspension were: 1, 3, 5, 7, 9, 11, and 13 and they did not vary significantly during the experiments. For a few runs different amounts of H_2O_2 or NaCl were added to the suspension at pH value of 7; the ratios between H_2O_2 or NaCl and phenol were 50 : 1 or 100 : 1 ($M : M$). The ferrioxalate actinometer method (19) was used for measuring the photon flow. The volume of the actinometer solution was always 40 cm^3. The absorbance of the actinometer samples was measured at the wavelength of 510 nm by using a Varian DMS 90 spectrophotometer.

The second series of runs allowed to determine the values of the kinetic constant of the photoreaction under investigation. The photoreactivity tests were carried out under the same experimental conditions as the actinometer runs by using a volume of suspension of 100 cm^3; the runs lasted 30 or 120 min depending on the light intensity used. The phenol concentration was determined using a standard colorimetric method (20) by withdrawing 3 cm^3 of suspension every 5 or 20 min depending on the duration of the run. It is worth reporting that the photoreactor was raised after each withdrawal in order to restore the initial distance of the top of the suspension from the collimating lenses.

The actinometer solution and the suspension were magnetically stirred at a speed that guaranteed a complete dispersion without the formation of a significant central vortex. The stirring speed was held constant during all the experiments (250 rpm) as the photon flow transmitted by the suspension and the photoactivity could depend on it (21). Three different stir bars of cylindrical shape (length: 13, 28, and 38 mm and diameter: 5, 6, and 8 mm, respectively) were immersed in the suspension in order to check the influence of their presence on the actinometer measurements. It was found that the photon flow transmitted by the suspension was insensitive to the stir bar dimensions. The photon flow incident in the suspension, Φ_i, was measured at equal reaction conditions but without suspended solids and stir bar in the photoreactor.

The "home prepared" (hp) polycrystalline TiO_2 catalyst was prepared in the following way. An amorphous precipitate was obtained by adding a 25% aqueous NH_3 solution (Merck, pro analysi) to a 15% $TiCl_3$ solution (Carlo Erba, RPE). Details of the procedure can be found elsewhere (22). Different fractions of the powder were heated at 773 K for 16, 48, or 168 h. Hereafter these powders are indicated as HP_{16}, HP_{48}, and HP_{168}, respectively. X-ray diffraction analysis revealed that the ther-

mal treatment produced only the anatase phase. Each portion of the catalyst was sieved in order to obtain samples with the following ranges of particle size: 210–250, 125–177, and 44–88 μm. The surface areas of the powders were determined by the dynamic BET method using a Micromeritics Flowsorb 2300 apparatus and N_2 as adsorbate.

Scanning electron microscopy was carried out using a Philips 505 microscope. Optical microscopy observation was carried out using a Euromex microscope. In order to check the mechanical resistance of the powder, microphotographs of the dried photocatalysts and of the same photocatalysts dispersed in water or in cyclohexane before and after stirring were obtained. The procedure for obtaining the microphotographs was the following. A beaker with the same dimensions as those of the photoreactor was used for performing some runs of stirring of different durations at the same agitation speed used for all the actinometer and reactivity experiments. At the end of the run, the suspended solid was allowed to settle while the supernatant water naturally evaporated at ambient temperature. After a few days the bottom of the beaker was covered by a dry layer of solid particles; this layer was then photographed.

RESULTS

The values of surface area (SA) for HP_{16}, HP_{48}, and HP_{168} powders are 60, 55, and 51 $m^2 \times g^{-1}$, respectively. The particle size does not affect the SA values while the increase of thermal treatment duration determines a decrease in the SA values. The SEM investigation shows that by increasing the duration of the thermal treatment the particles agglomerate and some sintering occurs. This behaviour can justify the small decrease of the surface areas.

Figure 1 reports the microphotographs performed for testing the mechanical resistance of the catalyst particles. Figure 1a shows the TiO_2 hp catalyst before its suspension and stirring in water. Figure 1b shows the same powder after a stirring for 30 min; it may be noted that the powder is scarcely affected by this treatment. For the sake of comparison a commercial TiO_2 (Merck) specimen of the same particle size range has been tested. Figure 1c shows the commercial specimen before the treatment; Fig. 1d shows the same specimen after its suspension in water and stirring for 30 s. It may be noted that the catalyst exhibits a very significant variation of the particle size even for a short time of stirring. By changing the solvent from water to cyclohexane, the TiO_2 hp showed the same behaviour as in water while the variation of particle size for commercial TiO_2 was less significant and may be ascribed essentially to stirring.

The rate of transmitted photon flow, Φ_0, was measured having the photoreactor filled with the suspension; typical experimental values for an incident photon flow of 275×10^{-8} einstein $\times s^{-1}$ are reported in Fig. 2. The measurement of Φ_0 was also used for checking the invariance of particle size after different times of stirring. It was found that the Φ_0 values did not change appreciably with stirring time. This behavior was exhibited by all the powders used.

The rate of backward reflected photons, Φ_r, was determined by the extrapolation method reported in Refs. (16) and (17). The method mainly consists in measuring the rate of transmitted photon flow as a function of the suspension volume, V. The following relationship was found to hold:

$$\Phi_0 = \Phi' \exp[-E \times C_{cat} \times V], \qquad [1]$$

Φ' being the rate of photons able to penetrate the suspension, E the apparent Napierian extinctance (ANE) coefficient of suspension, and C_{cat} the catalyst concentration. By applying a least-square best fitting procedure on the experimental data of Φ_0 vs V, the values of Φ' and E have been determined.

The application of a macroscopic photon balance on the photoreactor at the limit condition of $V = 0$, allows one to determine Φ_r:

$$\Phi_r = \Phi_i - \Phi'. \qquad [2]$$

For each photodegradation run the value of Φ_a, the photon flow absorbed by a suspension volume of 100 cm^3, was obtained by performing the following macroscopic photon balance on the photoreactor:

$$\Phi_a = \Phi_i - \Phi_o - \Phi_r. \qquad [3]$$

Table 1 reports the values of Φ', E, and R, the percentage of backward reflected photon flow, $R = (\Phi_r/\Phi_i) \times 100$, for HP_{16}, HP_{48}, and HP_{168} catalysts as a function of the incident photon flow and of the particle size for a suspension pH of 3. Table 2 reports the values of the previous quantities for HP_{48} catalyst as a function of the suspension pH and of the particle size for two different incident photon flows. Table 3 reports the values of these quantities for HP_{48} catalyst as a function of the particle size and of the molar ratio between H_2O_2 or NaCl and phenol at a suspension pH of 7 and an incident photon flow of 4.17×10^{-7} einstein $\times s^{-1}$.

The kinetics of phenol photodegradation are very complicated (12–15) as they depend on initial phenol concentration, oxygen and catalyst concentration, pH, ionic strength, radiation intensity, and generally by the physicochemical properties of the catalysts. For the experimental conditions imposed in the present work on the

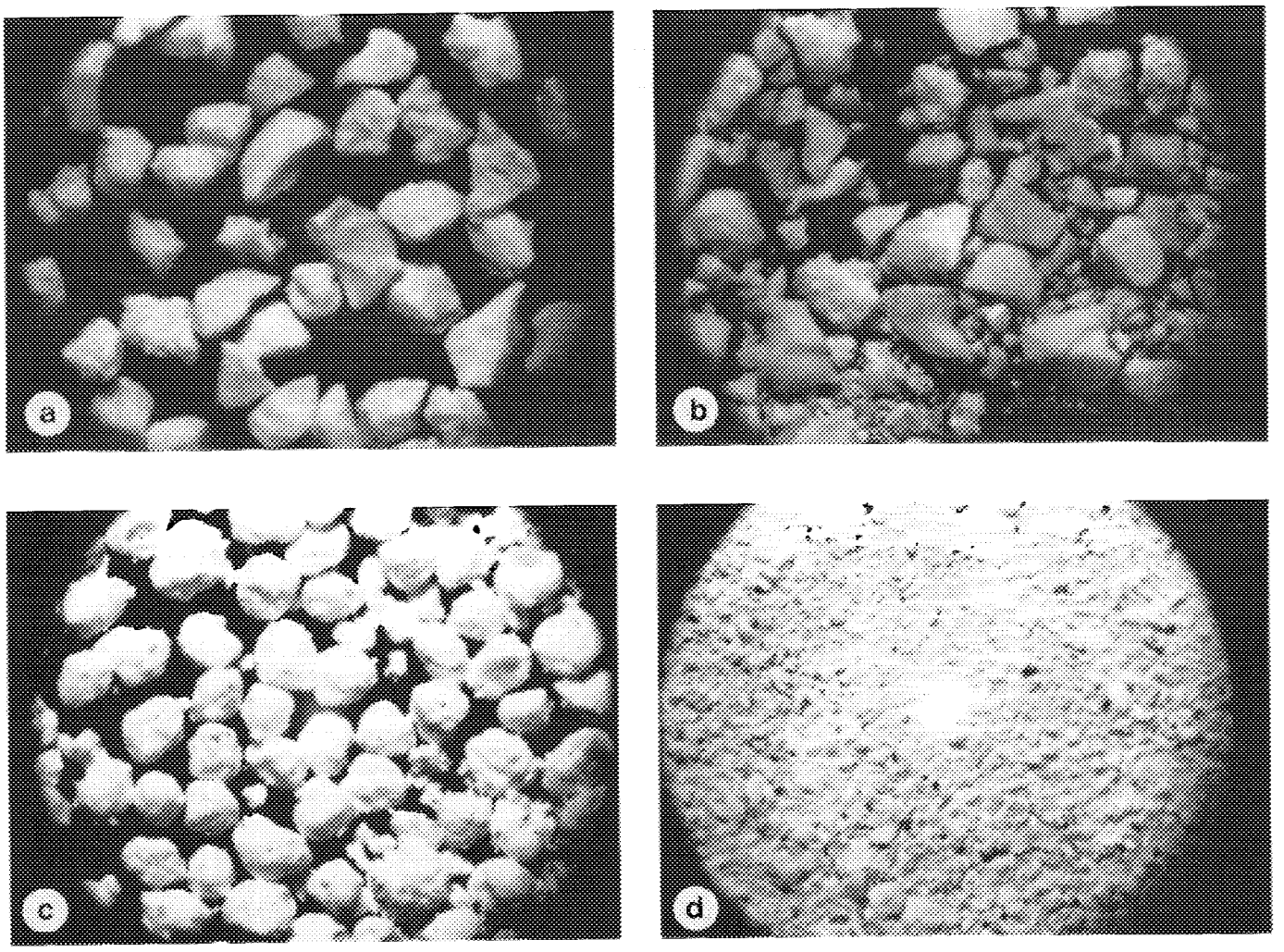

FIG. 1. Microphotographs (magnification × 40) performed for testing the mechanical resistance of the catalyst particles. (a) TiO_2 hp catalyst before suspension and stirring in water; (b) the same powder after a stirring for 30 min; (c) commercial TiO_2 specimen (Merck) before the treatment; (d) the same specimen after its suspension in water and stirring for 30 s.

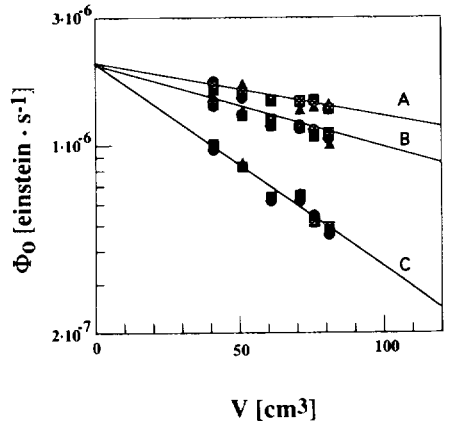

FIG. 2. Experimental values of transmitted photon flow, Φ_0, versus suspension volume, V, for HP_{16} (■), HP_{48} (●), and HP_{168} (▲). Incident photon flow of 275 × 10^{-8} einstein × s^{-1} and pH = 3. Particle size range: (A), 210–250 μm; (B), 125–177 μm; (C), 44–88 μm.

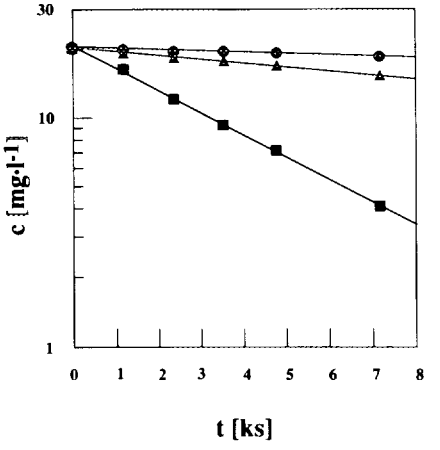

FIG. 3. Experimental values of phenol concentration, C, versus reaction time, t for HP_{48} catalyst at different incident photon flow. ●, 10.85 × 10^{-8} einstein × s^{-1}; ▲, 41.7 × 10^{-8} einstein × s^{-1}; and ■, 275 × 10^{-8} einstein × s^{-1}.

TABLE 1

Values of Φ', E, and R, the Percentage of Reflection, $(\Phi_r/\Phi_i) \times 100$, for HP_{16}, HP_{48} and HP_{168} Catalysts as a Function of Incident Photon Flow and Particle Size for a Suspension pH of 3

		210–250 μm			125–177 μm			44–88 μm		
Catalyst	$\Phi_i \times 10^8$ (einstein/s)	$\Phi' \times 10^8$ (einstein/s)	E (g^{-1})	R (%)	$\Phi' \times 10^8$ (einstein/s)	E (g^{-1})	R (%)	$\Phi' \times 10^8$ (einstein/s)	E (g^{-1})	R (%)
HP_{16}	10.85	8.28	3.02	23.7	8.28	4.46	23.7	8.28	9.51	23.7
HP_{48}	10.85	8.11	2.99	25.2	8.46	4.26	22	8.33	9.43	23.2
HP_{168}	10.85	8.45	3.04	22.1	8.33	4.38	23.2	8.41	9.39	22.5
HP_{16}	45.4	33.3	3.01	26.7	33.2	5.05	26.9	31.1	11.3	31.5
HP_{48}	45.4	35.4	3.08	22.1	30.6	4.36	32.6	32.6	9.43	28.2
HP_{168}	45.4	32.1	3.02	29.3	31.4	4.22	30.9	30.1	9.23	33.7
HP_{16}	275	205	3.28	25.6	212	4.86	22.9	208	9.55	24.3
HP_{48}	275	209	3.12	24.1	206	4.08	25.2	213	10.1	22.8
HP_{168}	275	210	3.21	23.7	208	4.36	24.4	207	9.13	24.8

reactivity runs; however, the photodegradation rate obeys a simple pseudo-first order kinetics. Typical reactivity results are reported in a semilogarithmic plot in Fig. 3 as phenol concentration versus reaction time. By applying a least-square best fitting procedure to the photoreactivity data of phenol concentration versus time, the values of the pseudo-first order rate constant, k_{obs}, were determined, and they are reported in Table 4 and in Fig. 4.

Table 4 reports the values of k_{obs} for HP_{16}, HP_{48}, and HP_{168} catalysts as a function of the incident photon flow and of the particle size for a suspension pH of 3. Figure 4 reports in a semilogarithmic plot the values for k_{obs} for HP_{48} catalyst as a function of the suspension pH and of the particle size for an incident photon flow of 4.17×10^{-7} einstein $\times$ s^{-1}; this figure also reports the value of k_{obs} obtained for runs performed at a pH value of 7 with a H_2O_2/C_6H_5OH molar ratio of 100.

Table 5 and Figure 5 report the calculated values of photoreaction quantum yield at the different experimental conditions used in this work; the figures of quantum yield, defined as the ratio between reacted molecules of phenol and photons absorbed by the suspension, were calculated in the following way. The number of phenol molecules reacted in the first 30 s of the runs was determined from the values of k_{obs} obtained from the reactivity experiments and the number of absorbed photons was obtained by applying the photon balance (Eq. [3]) to a suspension volume of 100 cm^3. It may be confidently assumed that at the start of the photodegradation runs only phenol molecules are present in the reacting mixture so that the aliquot of absorbed photons useful for the photo-

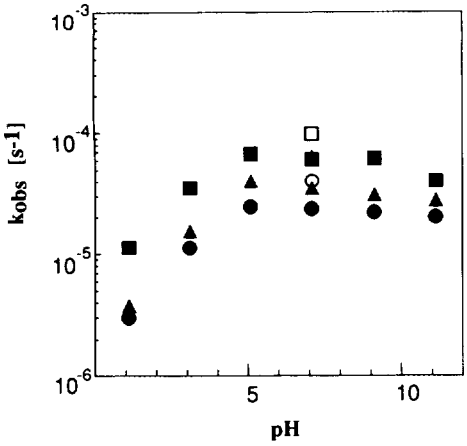

FIG. 4. Values of k_{obs} for HP_{48} catalyst as a function of suspension pH and particle size for an incident photon flow of 4.17×10^{-7} einstein $\times$ s^{-1}. Particle size range: ●, 210–250 μm; ▲, 125–177 μm; and ■, 44–88 μm. Empty symbols are relative to runs performed with a H_2O_2/C_6H_5OH ratio of 100 (M/M).

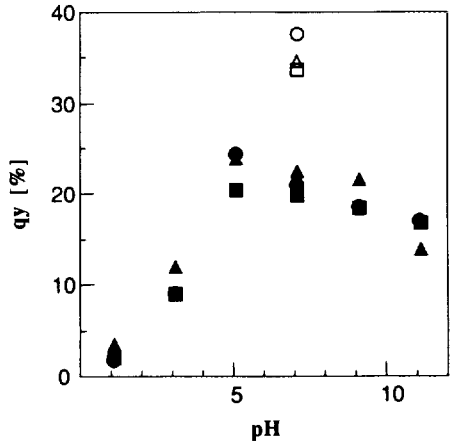

FIG. 5. Values of quantum yield as a function of suspension pH and particle size for an incident photon flow of 4.17×10^{-7} einstein $\times$ s^{-1}. Symbols as in Fig. 4.

TABLE 2

Values of Φ', E, and R, the Percentage of Reflection, $(\Phi_r/\Phi_i) \times 100$, for HP_{48} Catalysts as a Function of Suspension pH and Particle Size

		210–250 μm			125–177 μm			44–88 μm		
pH	$\Phi_i \times 10^8$ (einstein/s)	$\Phi' \times 10^8$ (einstein/s)	E (g^{-1})	R (%)	$\Phi' \times 10^8$ (einstein/s)	E (g^{-1})	R (%)	$\Phi' \times 10^8$ (einstein/s)	E (g^{-1})	R (%)
1	41.7	32.0	3.67	23.3	32.4	3.66	22.3	32.1	8.71	23.0
1	41.7	33.2	2.18	20.4	33.2	5.36	20.4	31.5	6.89	24.5
1	41.7	31.6	4.56	24.2	34.3	4.83	17.8	31.8	10.3	23.7
1	41.7	32.8	2.06	21.3	33.3	4.23	20.1	31.6	9.43	24.2
1	50.0	38.1	2.46	23.8	36.2	3.65	17.2	37.4	8.12	25.2
1	50.0	39.2	2.61	21.6	41.8	4.42	16.4	37.4	7.63	25.2
3	41.7	31.9	3.67	23.5	30.7	5.05	26.4	29.2	8.58	30.0
3	41.7	33.2	4.01	20.4	31.8	5.49	23.7	31.7	9.48	24.0
3	41.7	32.3	3.02	22.5	31.2	5.32	25.2	32.9	11.7	21.1
3	50.0	38.8	3.78	22.4	38.1	4.68	23.8	38.5	8.82	23.0
3	50.0	37.9	2.72	24.2	35.3	2.97	29.4	37.5	5.58	25.0
3	50.0	37.0	3.92	26.0	37.8	4.36	24.4	38.2	9.43	23.6
3	50.0	37.0	2.79	26.0	37.6	4.46	24.8	39.0	10.2	22.0
5	41.7	31.8	2.81	23.7	31.0	4.12	25.7	31.2	8.94	25.2
5	41.7	33.1	3.54	20.6	31.7	4.37	24.0	31.7	9.49	24.0
7	41.7	32.8	2.92	21.3	29.8	4.72	28.5	32.5	11.9	22.1
7	41.7	33.0	3.54	20.9	31.9	4.26	23.5	28.5	8.34	31.6
7	50.0	38.3	3.02	23.4	36.9	4.44	26.2	38.1	7.58	23.8
7	50.0	37.5	3.02	25.0	37.3	4.28	25.4	39.6	6.93	20.8
9	41.7	31.3	2.91	24.9	31.2	4.07	25.2	33.1	11.7	20.6
9	41.7	33.3	3.19	20.1	31.9	4.51	23.5	30.6	10.2	26.6
11	41.7	33.4	2.36	19.9	31.8	4.35	23.7	31.4	10.8	24.7
11	41.7	33.9	2.39	18.7	30.8	4.26	26.1	33.1	11.8	20.6
13	41.7	33.0	2.61	20.9	32.5	3.98	22.1	33.3	9.14	20.1
13	41.7	33.2	2.59	20.4	32.5	4.36	22.1	31.8	9.48	23.7
13	50.0	37.6	3.05	24.8	37.9	4.48	24.2	38.8	9.12	22.4
13	50.0	38.8	3.03	22.4	38.2	4.22	23.6	38.7	9.61	22.6

TABLE 3

Values of Φ', E, and R, the Percentage of Reflection, $(\Phi_r/\Phi_i) \times 100$, for HP_{48} Catalysts as a Function of Particle Size and Molar Ratio between H_2O_2 or NaCl and Phenol at a Suspension pH of 7 and an Incident Photon Flow of 4.17×10^{-7} einstein $\times$ s^{-1}

		210–250 μm			125–177 μm			44–88 μm		
$[H_2O_2]/[C_6H_5OH]$	$[NaCl]/[C_6H_5OH]$	$\Phi' \times 10^8$ (einstein/s)	E (g^{-1})	R (%)	$\Phi' \times 10^8$ (einstein/s)	E (g^{-1})	R (%)	$\Phi' \times 10^8$ (einstein/s)	E (g^{-1})	R (%)
100	—	31.2	2.99	25.2	30.7	3.85	26.4	31.2	9.66	25.2
100	—	31.1	2.82	25.4	31.7	4.21	24.0	31.8	9.44	23.7
50	—	31.0	2.84	25.7	30.5	4.04	26.9	33.3	12.2	20.1
—	100	30.5	2.93	26.9	33.2	4.74	20.4	32.6	7.68	21.8
—	50	30.6	2.78	26.6	31.5	4.09	24.5	31.6	10.2	24.2
—	50	32.2	3.21	22.8	31.9	4.36	23.5	30.8	9.37	26.1

reaction is utilized only for phenol degradation. Table 5 reports the values of qy as a function of the incident photon flow and of the particle size at a suspension pH of 3. Figure 5 reports in a linear plot the values of qy as a function of the suspension pH and of the particle size for an incident photon flow of 4.17×10^{-7} einstein $\times$ s^{-1}; this figure also reports the value of qy obtained for the runs performed at a pH value of 7 with a H_2O_2/C_6H_5OH molar ratio of 100.

DISCUSSION

From the data of Φ', E, and R reported in Tables 1–3 the following considerations on the optical properties of TiO_2 suspensions can be drawn:

(i) at equal range of particle size, the values of the apparent Napierian extinction coefficient are independent of variables investigated in the present work, i.e., the surface area of the photocatalyst, incident radiation flow, pH of the suspension, presence of substances which increase (H_2O_2) or decrease (NaCl) the photoreactivity;

(ii) the values of E increase as a result of decreasing the particle size;

(iii) the percentage of reflection, R, is an intrinsic parameter of the solid material as it does not depend on any of the operative variables changed in the course of this work.

The theory of radiative transfer in scattering and absorbing media (23, 24) indicates that, for particles of size greater than the wavelength, the scattering phenomenon is mainly a reflection process and hence it can be treated by using simple geometrical reflection relations. From the Kubelka–Munk theory (25) the scattering coefficient in the case of diffuse incident irradiation of "dilute" systems is inversely proportional to the average grain size. Figure 6 reports the mean value of the apparent Napierian extinctance, E, as a function of the inverse of the average particle size, d. A straight line fits satisfactorily the experimental data thus indicating that the ANE shows the same dependence on the particle size as that shown by the scattering coefficient. This feature indicates that the ANE, which was introduced only as a phenomenological parameter, can be confidently assumed as a reliable parameter for characterizing the optical behavior of solid suspensions of large particles.

It must be reported that in a previous paper (16) the apparent Napierian extinctance was found to be independent of the particle size. The origin of this statement was the use for the experimental runs performed in that work of a commercial TiO_2 (Merck) specimen which does not retain the particle size, as has been found in the present work.

The reactivity data reported in Table 4 and Fig. 4 suggest the following considerations:

(i) the values of pseudo-first order rate constant, k_{obs}, at a fixed pH value, do not depend on the surface area of the photocatalyst; they increase by increasing the incident photon flow and by decreasing the particle size;

TABLE 4

Values of k_{obs} for HP_{16}, HP_{48}, and HP_{168} Catalysts as a Function of Incident Photon Flow and Particle Size for a Suspension pH of 3

Catalyst	$\Phi_i \times 10^8$ (einstein/s)	210–250 μm $k_{obs} \times 10^6$ (s^{-1})	125–177 μm $k_{obs} \times 10^6$ (s^{-1})	44–88 μm $k_{obs} \times 10^6$ (s^{-1})
HP_{16}	10.85	3.7	5.25	9.3
HP_{48}	10.85	3.4	5.08	8.7
HP_{168}	10.85	3.5	5.12	9.0
HP_{48}	41.7	12.3	17.0	38.3
HP_{16}	45.4	12.8	21.3	32.7
HP_{48}	45.4	13.6	21.2	31.2
HP_{168}	45.4	12.4	20.8	33.7
HP_{16}	275	90.5	132.5	221.8
HP_{48}	275	91.8	133.9	220.2
HP_{168}	275	89.7	130.1	221.2

TABLE 5

Values of Quantum Yield as a Function of Incident Photon Flow and Particle Size for a Suspension pH of 3

$\Phi_i \times 10^8$ (einstein/s)	210–250 μm qy $\times 10^2$	125–177 μm qy $\times 10^2$	44–88 μm qy $\times 10^2$
10.85	10.51	11.23	11.41
41.7	9.49	9.64	12.62
45.4	9.14	10.98	9.86
275	10.57	11.34	10.97

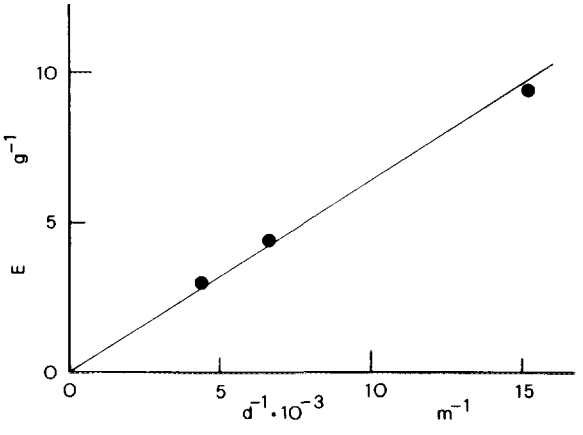

FIG. 6. The mean values of the apparent Napierian extinctance, E, versus the inverse of the average particle size.

(ii) the values of k_{obs} for powders of equal particle size increase when the pH changes from acid to neutral values. A maximum of reactivity is exhibited in the 5–7 pH range. By increasing the pH in the basic region the reactivity decreases smoothly. The presence of hydrogen peroxide in the suspension increases the reactivity by a factor of about 2.

The photoreactivity results are in good agreement with the literature (12–15); in the presence of H_2O_2, moreover, a significant increase of the photodegradation rate of phenol in aqueous TiO_2 suspensions has been reported (26). Indeed, the concentration of highly reactive species, responsible for the oxidative attack on the organic substrate, increases in the presence of H_2O_2 according to the following reactions:

$$H_2O_{2(ads)} + e^-_{CB} \rightarrow OH^- + OH^{\cdot} \quad [4]$$

$$H_2O_{2(ads)} + h^+_{VB} \rightarrow H^+ + HO_2^{\cdot}. \quad [5]$$

For heterogeneous photocatalytic reactions the dependence of the kinetic constant, k, on the radiation intensity has been reported (27) to be a power law relationship of the form: $k = k(\Phi^p)$ in which p ranges from 0.5 to 1. At low light intensities a linear dependence of k on Φ is found while at high intensities a square-root dependence arises. A likely explanation of this behavior is that at increasing electron-hole generation rate (determined by the high radiation intensities) there is the predominance of the rate of electron-hole recombination with respect to the rate of electron-hole capture by species involved in the chemical reaction. For determining in which region the photoprocess under investigation is occurring, the values of k_{obs} have been plotted against the mean value of radiation intensity inside the reacting medium. By considering that the radiation intensity inside the reacting medium decreases by following the relationship given by Eq. [1], the mean value of Φ for a reactor volume of 100 cm^3 is given by

$$\Phi_{mean} = \Phi'[1 - \exp(-100 \times E \times C_{cat})]/(100 \times E \times C_{cat}). \quad [6]$$

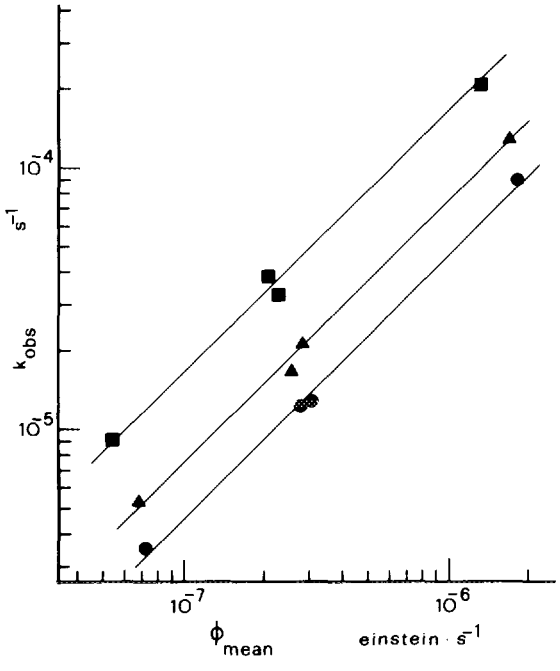

FIG. 7. The values of the kinetic constant, k_{obs}, versus the mean radiation intensity, Φ_{mean}. Symbols as in Fig. 4.

Figure 7 reports in a logarithmic plot the values of k_{obs} vs Φ_{mean} for each particle size. There is a satisfactory fit to a straight line thus indicating that under the used experimental conditions the photon flow is limiting the reaction rate. It must also be noted that a plot of k_{obs} vs Φ_i may give erroneous indications.

Table 5 and Fig. 5 report the calculated values of the quantum yield of the photoprocess. By considering that the values of k_{obs} reported in Table 4 do not depend on the duration of the thermal treatment, the corresponding values of quantum yield, reported in Table 5, have been determined by using the mean values of the kinetic constant for calculating the reacted molecules of phenol. On the same ground the values of quantum yield reported in Fig. 5 as a function of the suspension pH, have been determined by using the mean value of E and of Φ' for calculating the absorbed photons.

The values of quantum yield reported in Table 5 and Fig. 5 clearly indicate that the quantum yield of photoreaction is independent of the particle size and it is affected only by the pH of the suspension or by the presence of species as H_2O_2 influencing the photoreactivity. It must be noted, however, that the variations of quantum yield with the pH or in the presence of H_2O_2 are determined only by a variation of the reactivity while the amount of photons absorbed by the solid suspension is unaffected.

CONCLUSIONS

The optical properties of TiO_2 suspensions, in the experimental conditions used in the present paper, can be summarized as follows:

(i) the apparent Napierian extinction coefficient depends only on the particle size; the average values of E obtained in the present work are 3.04, 4.39, and 9.42 g^{-1} for particles in the 210–250, 125–177, and 44–88 μm size range, respectively;

(ii) the percentage of reflection of the TiO_2 suspension, whose mean value is 23.76%, is a feature of material as it is independent of any environmental parameter;

(iii) the absorption of photons by the solid can be affected only by changing the particle size. In this way the reaction rate of a photocatalytic process can be increased but the quantum yield remains constant.

ACKNOWLEDGMENTS

The authors thank the referees for valuable and helpful suggestions. Financial support from the "Ministero dell'Universitá e della Ricerca Scientifica e Tecnologica" (MURST, Rome) is also gratefully acknowledged.

REFERENCES

1. Schiavello, M. (Ed.), "Photoelectrochemistry, Photocatalysis and Photoreactors. Fundamentals and Developments." Reidel, Dordrecht, 1985.
2. Schiavello, M. (Ed.), "Photocatalysis and Environment. Trends and Applications." Kluwer, Dordrecht, 1988.
3. Serpone, N., and Pelizzetti, E. (Eds.), "Photocatalysis. Fundamentals and Applications." Wiley, New York, 1989.
4. Childs, L. P., and Ollis, D. F., *J. Catal.* **66,** 383 (1988).
5. Kisch, H., *in* "Photocatalysis. Fundamentals and Applications" (N. Serpone and E. Pelizzetti, Eds.). Wiley, New York, 1989.
6. Palmisano, L., Augugliaro, V., Campostrini, R., and Schiavello, M., *J. Catal.* **143,** 149 (1993).
7. Augugliaro, V., Schiavello, M., and Palmisano, L., *Coord. Chem. Rev.* **125,** 173 (1993).
8. Serpone, N., Terzian, R., Lawless, D., Kennepohl, P., and Sauve, G., *J. Photochem. Photobiol. A Chem.* **73,** 11 (1993).
9. Ollis, D. F., and Al-Ekabi, H. (Eds.), "Photocatalytic Purification and Treatment of Water and Air," Elsevier, Amsterdam, 1993.
10. Zhang, Y., Crittenden, J. C., Hand, D. W., and Perram, D. L., *Environ. Sci. Technol.* **28,** 435 (1994).
11. Hofstadler, K., Bauer, R., Novalic, S., and Heisler, G., *Environ. Sci. Technol.* **28,** 670 (1994).
12. Okamoto, K., Yamamoto, Y., Tanaka, H., Tanaka, M., and Itaya, A., *Bull. Chem. Soc. Jpn.* **58,** 2015 (1985).
13. Okamoto, K., Yamamoto, Y., Tanaka, H., and Itaya, A., *Bull. Chem. Soc. Jpn.* **58,** 2023 (1985).
14. Augugliaro, V., Palmisano, L., Sclafani, A., Minero, C., and Pelizzetti, E., *Toxicol. Environ. Chem.* **16,** 89 (1988).
15. Matthews, R. W., and McEvoy, S. R., *J. Photochem. Photobiol. A Chem.* **64,** 231 (1992).
16. Augugliaro, V., Palmisano, L., and Schiavello, M., *AIChE J.* **37,** 1096 (1991).
17. Schiavello, M., Augugliaro, V., and Palmisano, L., *J. Catal.* **127,** 332 (1991).
18. Martín, C. A., Baltanás, M. A., and Cassano, A. E., *J. Photochem. Photobiol. A Chem.* **76,** 199 (1993).
19. Murov, S. L. (Ed.), "Handbook of Photochemistry," p. 119. Dekker, New York, 1973.
20. Taras, H. J., Greenberg, A. E., Hoak, R. D., and Rand, M. C. (Eds.), "Standard Methods for the Examination of Water and Wastewater" Am. Public Health Assoc., Washington DC, 1971.
21. Karakitsou, K. E., and Verykios, X. E., *J. Catal.* **134,** 629 (1992).
22. Sclafani, A., Palmisano, L., and Schiavello, M., *J. Phys. Chem.* **94,** 829 (1990).
23. van de Hulst, H. C., "Light Scattering by Small Particles," Dover, New York, 1981.
24. Bohren, C. F., and Huffman, D. R., "Absorption and Scattering of Light by Small Particles," Wiley, New York, 1983.
25. Kortüm, G., "Reflectance Spectroscopy," Springer-Verlag, Berlin, 1969.
26. Augugliaro, V., Davì, E., Palmisano, L., Schiavello, M., and Sclafani, A., *Appl. Catal.* **65,** 101 (1990).
27. Pichat, P., *in* "Photoelectrochemistry, Photocatalysis and Photoreactors. Fundamentals and Developments" (M. Schiavello, Ed.), p. 425. Reidel, Dordrecht, 1985.